



Trans. Nonferrous Met. Soc. China 22(2012) 2021-2026

Transactions of Nonferrous Metals Society of China

www.tnmsc.cn

# Thermal stability and Judd-Ofelt analysis of optical properties of Er<sup>3+</sup>-doped tellurite glasses

REN Fang, MEI Yu-zhao, GAO Chao, ZHU Li-gang, LU An-xian School of Materials Science and Engineering, Central South University, Changsha 410083, China Received 6 September 2011; accepted 10 January 2012

**Abstract:** Er<sup>3+</sup>-doped TeO<sub>2</sub>–ZnO–Na<sub>2</sub>O–B<sub>2</sub>O<sub>3</sub>–GeO<sub>2</sub> (TZNBG) glasses were prepared by melt-quenching method. Differential scanning calorimetry (DSC) and thermal mechanical analysis (TMA) were used to calculate thermal parameters: crystallization temperature ( $T_x$ ), glass transition temperature ( $T_y$ ) and thermal expansion (α). Besides, Judd-Ofelt theory is applied to analyzing absorption spectra. Intensity parameters  $\Omega_\lambda$  ( $\lambda$ =2, 4, 6), transition probabilities  $A_{ed}$ , radiative lifetime  $\tau_i$ , and branching ratios  $\beta$  of Er<sup>3+</sup> transitions were obtained. Emission cross-section  $\sigma_{emis}$  of  ${}^4I_{13/2}$ — ${}^4I_{15/2}$  transition of Er<sup>3+</sup> was calculated according to the theory of McCumber. All of the parameters indicate that the thermal stability and optical properties of Er<sup>3+</sup>-doped TZNBG glasses are improved effectively.

**Key words:** tellurite glasses; thermal stability; Judd-Ofelt theory; spectroscopic properties

#### 1 Introduction

Er<sup>3+</sup>-doped tellurite glasses possess large emission cross-section, flattened broad bandwidth, excellent transmission in visible and near IR, relatively low phonon energy and a large refractive index compared with other oxide glasses [1,2]. Due to their excellent properties, the Er<sup>3+</sup>-doped tellurite glasses are used as candidates for broad band amplifiers [3,4]. But, serious drawback for tellurite glasses is their relatively low thermal stability. These disadvantages result in that fibers made from these glasses are too fragile, so they do not show light guiding at all [5]. Furthermore, the tellurite glasses are hard to applicate due to their drawbacks. And so far there are many studies about improving their thermal stability. JLASSI et al [6] reported that both thermal stability and quantum efficiency were improved by adding P2O5 to tellurite glasses. EL-MALLAWANY et al [7] made quantitative analysis of thermal properties of tellurite glass with the structure parameters like the average cross-link density, the number of bonds per unit volume, and the average stretching force constant, but the optical properties were not reported. It is necessary to possess excellent thermal stability for the tellurite glasses for further application in optical fiber amplifiers.

In this work, improving thermal stability and optical properties is the main purpose. The Er³+-doped TeO<sub>2</sub>–ZnO–Na<sub>2</sub>O–B<sub>2</sub>O<sub>3</sub>–GeO<sub>2</sub> (TZNBG) glasses were elaborated by melt-quenching method. Both B<sub>2</sub>O<sub>3</sub> and GeO<sub>2</sub> introduced into tellurite glass compositions at the same time have been rarely reported. And differential scanning calorimetry (DSC), thermal mechanical analysis (TMA), absorption and emission measurements were performed. In addition, theories of Judd-Ofelt and McCumber were applied to analyzing the optical properties.

#### 2 Experimental

Tellurite glasses with compositions listed in Table 1 were prepared. Er<sub>2</sub>O<sub>3</sub> (99.95%, mass fraction) was added into all glass samples. Na<sub>2</sub>O and B<sub>2</sub>O<sub>3</sub> were introduced in the form of Na<sub>2</sub>CO<sub>3</sub> and H<sub>3</sub>BO<sub>3</sub>, respectively. Batches of 15 g were prepared from commercial powders of TeO<sub>2</sub> (99.999%), ZnO (99.9%), Na<sub>2</sub>CO<sub>3</sub> (99.9%), H<sub>3</sub>BO<sub>3</sub> (99.9%) and GeO<sub>2</sub> (99.99%). The powders were mixed in a mortar and immersed in CCl<sub>4</sub> which was as a reagent of dehydration for 10 min at room temperature. The homogeneous mixture was melted in an alumina crucible at 600 °C for 0.5–1 h, then at 900 °C for 1–2 h in a furnace. When the melting was completed, the liquids

**Table 1** Compositions of Er<sup>3+</sup>-doped tellurite glasses

| Glass<br>sample | x(TeO <sub>2</sub> )/ | x(Na <sub>2</sub> O)/ % | x(ZnO)/<br>% | x(B <sub>2</sub> O <sub>3</sub> )/ | x(GeO <sub>2</sub> )/ |
|-----------------|-----------------------|-------------------------|--------------|------------------------------------|-----------------------|
| TZN             | 70                    | 10                      | 20           |                                    |                       |
| TZNBG 1         | 50                    | 10                      | 20           | 15                                 | 5                     |
| TZNBG 2         | 50                    | 10                      | 15           | 20                                 | 5                     |
| TZNBG 3         | 50                    | 10                      | 10           | 25                                 | 5                     |
| TZNBG 4         | 50                    | 10                      | 0            | 35                                 | 5                     |

1% Er<sub>2</sub>O<sub>3</sub> was added into all glass samples.

were poured into preheated massive graphite plates at 300–320 °C and annealed at this temperature for 3 h. The glasses were cooled to 100 °C after 24 h. The glass blocks prepared were cut into desired dimensions and optically polished for different measurements.

Thermal analysis was performed with a TAS100 thermal analytical instrument and Netzsch DTA 449 PC differential scanning calorimeter at a heating rate of 10 °C/min. The absorption spectra were recorded by a Perkin-Elmer Lambda–900 spectrophotometer in the wavelength range of 400–1700 nm. And emission spectra were collected by using Edinburgh Instruments Ltd FLSP 920 spectrophotometer, with 976 nm laser diode as the excitation source. Glass samples for optical and spectroscopic measurements were cut and polished in the demensions of 15 mm×15 mm×3 mm and all the optical measurements were carried out at room temperature.

#### 3 Results and discussion

### 3.1 Thermal stability

In order to evaluate the thermal stability of glass samples, measurements of DSC and TMA were performed. Figure 1 presents the DSC curve of TZNBG glasses. The DSC curve shows glass transition temperature  $(T_g)$  and crystallization temperature  $(T_x)$  in glass sample. And thermal expansion coefficient  $\alpha$  was obtained by TMA. Results of thermal parameters are listed in Table 2.  $\Delta T$  is identified as:  $\Delta T = T_x - T_g$ . And the  $\Delta T$  has been frequently used as a rough measure of the glass thermal stability [8]. Since fiber fabricating is a reheating process, any crystallization during the process will lead to more scattering loss of the fiber and then damage the optical properties. To achieve a large range of working temperature during the fiber fabricating and to obtain glass fiber with superior optical properties, it is desired that  $\Delta T$  of glass as large as possible [9]. The  $T_{\rm g}$ and glass softening temperature  $(T_f)$  increase for the B<sub>2</sub>O<sub>3</sub> and GeO<sub>2</sub> introduced into glass compositions. And the crystallization peaks were extremely weak in samples of TZNBG glass. Furthermore, the value of  $\Delta T$  is larger than 134 °C. In addition,  $\alpha$  of TZNBG glass samples is in the range of  $(10.938-12.279)\times 10^{-6}$ ° C<sup>-1</sup>. It is much lower than  $15.466\times 10^{-6}$ ° C<sup>-1</sup> of TZN glass sample. So, it suggests that introducing  $B_2O_3$  and  $GeO_2$  into tellurite glasses can improve their thermal stability. The reason for the performance change is structure of glass changed after introducing  $B_2O_3$  and  $GeO_2$  into the tellurite glasses [4].

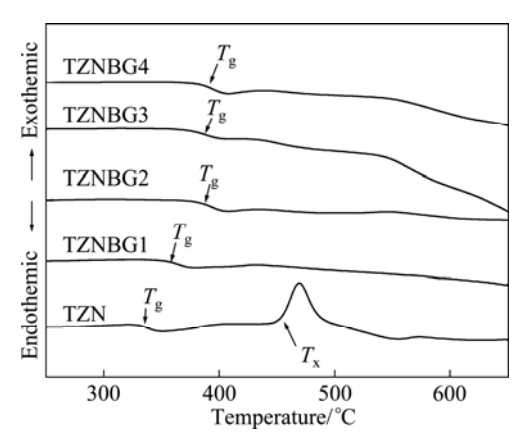


Fig. 1 DSC curves of glass sample

Table 2 Thermal parameters of different glass samples

| Glass sample           | $T_{\rm g}/$ °C | T <sub>x</sub> / °C | <i>T</i> <sub>f</sub> / °C | $\alpha/(10^{-6} \text{ C}^{-1})$ | Δ <i>T</i> /<br>°C |
|------------------------|-----------------|---------------------|----------------------------|-----------------------------------|--------------------|
| TZN (Present work)     | 335             | 469                 | 353                        | 15.466                            | 134                |
| TZNBG 1 (Present work) | 363             | *                   | 388                        | 12.279                            | _                  |
| TZNBG 2 (Present work) | 388             | *                   | 423                        | 10.938                            | _                  |
| TZNBG 3 (Present work) | 380             | *                   | 416                        | 11.479                            | _                  |
| TZNBG 4 (Present work) | 392             | *                   | 421                        | 11.286                            | _                  |
| TZNE 1 [6]             | 316             | 456                 |                            |                                   | 140                |
| BT-70 [10]             | 623             | 715                 |                            |                                   | 92                 |
| BT-60 [10]             | 625             | 700                 |                            |                                   | 75                 |
| BT-50 [10]             | 592             | 670                 |                            |                                   | 78                 |

<sup>&</sup>quot;\*" indicates that DSC curve of glass sample has no obvious crystallization neak

#### 3.2 Absorption spectra and Judd-Ofelt analysis

The TZNBG 2 glass sample was selected for further optical studies due to its relatively good thermal stability, and the TZN sample was as comparison.

Figure 2 illustrates the absorption spectra of  $Er^{3+}$ -doped TZNBG 2 and TZN glass samples. The absorption spectra consist of eight absorption bands at 1531, 978, 796, 652, 544, 521, 488 and 451 nm, corresponding to the absorption from the ground state  ${}^4I_{15/2}$  to the excited sates of  ${}^4I_{13/2}$ ,  ${}^4I_{11/2}$ ,  ${}^4I_{9/2}$ ,  ${}^4F_{9/2}$ ,  ${}^4F_{3/2}$ ,  ${}^2H_{11/2}$ ,  ${}^4F_{7/2}$  and  ${}^4F_{5/2}$  of  $Er^{3+}$ , respectively. As we can see the peak position of each transition remains unchanged with adding the  $B_2O_3$  and  $GeO_2$ .

The theory of Judd-Ofelt [11,12] is often used to calculate the spectroscopic parameters such as oscillator coefficient f, intensity parameters  $\Omega_{\lambda}$  ( $\lambda$ =2, 4, 6),

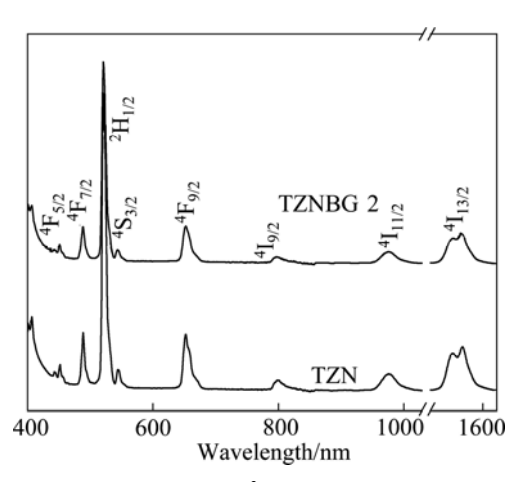


Fig. 2 Absorption spectra of Er<sup>3+</sup>-doped tellurite glasses

transition probability  $A_{\rm ed}$ , branching ratio  $\beta$ , radiative lifetime  $\tau_i$ . The oscillator coefficient for each band is computed by the following expression:

$$f_{\rm exp} = \frac{2303mc^2}{N\pi e^2} \int \varepsilon(\sigma) d\sigma = 4.318 \times 10^{-9} \int \varepsilon(\sigma) d\sigma \qquad (1)$$

where N is the number of rare earth ions per unit volume;  $\varepsilon(\sigma)$  is the molar absorptivity in L/(mol·cm) of band at a mean energy  $\sigma$  in cm<sup>-1</sup>, which is computed from the measured absorbance for known concentrations  $N_0$  of the Er in the glass [13].

According to the Judd-Ofelt theory the oscillator strength of an electric dipole transition  $(S, L, J \rightarrow S', L', J')$  is determined from formula (2):

$$f_{\text{cal}} = \frac{8\pi^2 mc}{3h(2J+1)} \frac{(n^2+2)^2}{9n} \sigma \cdot \sum_{\lambda=2,4,6} \Omega_{\lambda} \left| \left\langle (SLJ) \parallel U^{(\lambda)} \parallel (S'L'J') \right\rangle \right|^2$$
(2)

where h is the Planck's constant; c is the speed of light; m is the mass of electron; n is the refractive index;  $U(\lambda) = \left| \left\langle (SLJ) \right| \mid U^{(\lambda)} \mid \mid (S'L'J') \right\rangle \right|$  is the doubly reduced unit tensor operator that is taken from Ref. [13]. The Judd-Ofelt parameters  $\Omega_{\lambda}$  ( $\lambda$ =2, 4, 6) are obtained by a least-square method and the oscillator strength f for any transition is evaluated from formula (2). The quality of the fitting of the theoretical oscillator strength values to the measured ones can be expressed by the root-mean-square  $\delta_{\rm rms}$ , which is calculated by:

$$\delta_{\rm rms} = \left\lceil \frac{\sum (f_{\rm cal} - f_{\rm exp})^2}{N_{\rm bnads} - 3} \right\rceil^{1/2} \tag{3}$$

where  $N_{\text{bands}}$  regards the number of transition bands analyzed.

The values of  $\Omega_{\lambda}$  ( $\lambda$ =2, 4, 6) can be applied to calculating the radiative transition probabilities  $A_{\rm ed}$  ( $J' \rightarrow J''$ ), for excited levels of rare earth ions from an

initial state J' to a final ground state J'', is given by the following formula:

$$A_{\text{ed}}(J' \to J'') = \frac{64\pi^4 e^2 \sigma^3}{3h(2J'+1)} \frac{n(n^2+2)^2}{9} \cdot \sum_{\lambda=2,4,6} \Omega_{\lambda} \left| \left\langle (S'L'J') \parallel U^{(\lambda)} \parallel (S''L''J'') \right\rangle \right|^2$$
(4)

The total transition probability  $(A_{\rm T})$  has been evaluated from  $A_{\rm T} = \sum A_{\rm ed}$ . The branching ratio can be identified as  $\beta = A_{\rm ed}/A_{\rm T}$ . The radiative lifetime  $\tau_{\rm i}$  was calculated from  $\tau_{\rm i} = 1/A_{\rm T}$ . The oscillator strength f and the intensity parameter  $(\Omega_{\lambda})$  are set out in Table 3, and radiative transition probability  $(A_{\rm ed})$ , branching ration  $(\beta)$  and the radiative lifetime  $(\tau_{\rm i})$  are listed in Table 4.

**Table 3** Measured  $(f_{mea})$  and calculated  $(f_{cal})$  oscillator coefficient and intensity parameter  $(\Omega_{\lambda})$  for  $\mathrm{Er}^{3+}$ - doped tellurite glasses by Judd-Ofelt theory

| T  | λ/nm | TZ                    | ΣN                    | TZNBG 2                          |                       |  |
|--|------|-----------------------|-----------------------|----------------------------------|-----------------------|--|
| Transition                                 |      | $f_{\rm mea}/10^{-6}$ | $f_{\rm cal}/10^{-6}$ | $f_{\rm mea}/10^{-6}$            | $f_{\rm cal}/10^{-6}$ |  |
| $^{4}I_{15/2} \rightarrow ^{4}I_{13/2}$    | 1531 | 1.332                 | 1.215                 | 0.961                            | 0.8.79                |  |
| $^{4}I_{15/2} \rightarrow ^{4}I_{11/2}$    | 978  | 0.450                 | 0.611                 | 0.333                            | 0.440                 |  |
| $^{4}I_{15/2} \rightarrow ^{4}I_{9/2}$     | 796  | 0.239                 | 0.225                 | 0.220                            | 0.154                 |  |
| $^{4}I_{15/2} \rightarrow ^{4}F_{9/2}$     | 652  | 1.656                 | 1.611                 | 1.140                            | 1.134                 |  |
| $^{4}I_{15/2} \rightarrow ^{4}S_{3/2}$     | 544  | 0.348                 | 0.465                 | 0.221                            | 0.341                 |  |
| $^{4}I_{15/2} \rightarrow ^{2}H_{11/2}$    | 521  | 7.929                 | 7.932                 | 5.432                            | 5.426                 |  |
| $^{4}I_{15/2} \rightarrow ^{4}F_{7/2}$     | 488  | 1.258                 | 1.764                 | 0.921                            | 1.272                 |  |
| ${}^{4}I_{15/2} \rightarrow {}^{4}F_{5/2}$ | 451  | 0.255                 | 0.566                 | 0.205                            | 0.4.15                |  |
| $\delta_{\rm rms}/10^{-7}$                 |      | 2.8                   | 55                    | 2.023                            |                       |  |
| $\Omega_2/10^{-20}\mathrm{cm}^2$           |      | 5.757                 |                       | 5.018                            |                       |  |
| $\Omega_4/10^{-20} {\rm cm}^2$             |      | 1.106                 |                       | 0.949                            |                       |  |
| $\Omega_6/10^{-20} \text{cm}^2$            |      | 1.299                 |                       | 1.212                            |                       |  |
| Trend                                      |      | $\Omega_2 > \Omega_2$ | $Q_6 > \Omega_4$      | $\Omega_2 > \Omega_6 > \Omega_4$ |                       |  |
| $N_0/10^{22} \text{cm}^{-3}$               |      | 2.3                   | 52                    | 1.404                            |                       |  |

According to the theory of JACOBS and WEBER [14], erbium emission intensity can be characterized by  $\Omega_4$  and  $\Omega_6$  parameters. The smaller value of  $\Omega_4/\Omega_6$  corresponds to higher intensity of laser transition  ${}^4I_{13/2} \rightarrow {}^4I_{15/2}$  of Er<sup>3+</sup> [15]. In the present work, the value of  $\Omega_4/\Omega_6$  is estimated to be 0.783 for Er<sup>3+</sup> in TZNBG 2 glass sample, which indicates that the transition  ${}^4I_{13/2} \rightarrow {}^4I_{15/2}$  is more efficient than that in other glass samples [6,10,10]. The values of  $\Omega_4/\Omega_6$  of different glass samples are included in Table 5.

#### 3.3 Emission spectra and emission cross-section

Figure 3 exhibits the emission spectra for the  ${}^{4}I_{13/2} \rightarrow {}^{4}I_{15/2}$  transition of  $Er^{3+}$ -doped TZN and TZNBG 2 glass samples. According to the McCumber theory [17], the emission cross-section  $\sigma_{emis}$  can be determined by

**Table 4** Radiative transition probability  $(A_{ed})$ , branching ratio  $(\beta)$  and radiative lifetime  $(\tau_i)$  of energy levels of  $Er^{3+}$ -doped in tellurite glasses

| Transition   | TZN                                |                            |                        | TZNBG 2 |                                    |                            |                        |       |
|--|------------------------------------|----------------------------|------------------------|---------|------------------------------------|----------------------------|------------------------|-------|
|  | Average frequency/cm <sup>-1</sup> | $A_{\rm ed}/{\rm ns}^{-1}$ | $\tau_{\rm i}/{ m ms}$ | β/%     | Average frequency/cm <sup>-1</sup> | $A_{\rm ed}/{\rm ns}^{-1}$ | $\tau_{\rm i}/{ m ms}$ | β/%   |
| $^{4}I_{13/2} \rightarrow ^{4}I_{15/2}$  | 6545                               | 129.903                    | 7.698                  | 1.000   | 6552                               | 84.709                     | 11.805                 | 1.000 |
| ${}^{4}I_{11/2} \rightarrow {}^{4}I_{15/2}$  | 10232                              | 159.641                    | 5.544                  | 0.885   | 10225                              | 102.026                    | 8.681                  | 0.886 |
| $\frac{{}^{4}I_{13/2}}{{}^{4}I_{9/2} {}^{4}I_{15/2}}$  | 3686                               | 20.721                     |                        | 0.115   | 3673                               | 13.165                     |                        | 0.114 |
| $^{4}I_{9/2} \rightarrow ^{4}I_{15/2}$   | 12471                              | 87.414                     | 9.094                  | 0.795   | 12532                              | 52.823                     | 15.005                 | 0.793 |
| $\rightarrow$ <sup>4</sup> $I_{13/2}$  | 5925                               | 19.734                     |                        | 0.179   | 5980                               | 12.029                     |                        | 0.181 |
| $\rightarrow$ <sup>4</sup> $I_{11/2}$  | 2239                               | 2.818                      |                        | 0.026   | 2308                               | 1.791                      |                        | 0.027 |
| ${}^{4}\text{F}_{9/2} \rightarrow {}^{4}\text{I}_{15/2}$   | 15303                              | 941.410                    | 0.722                  | 0.680   | 15322                              | 590.610                    | 1.151                  | 0.680 |
| $\rightarrow$ <sup>4</sup> $I_{13/2}$  | 8757                               | 308.299                    |                        | 0.223   | 8770                               | 193.507                    |                        | 0.223 |
| $\rightarrow$ <sup>4</sup> $I_{11/2}$  | 5071                               | 103.380                    |                        | 0.075   | 5098                               | 65.369                     |                        | 0.075 |
| $\rightarrow$ <sup>4</sup> $I_{9/2}$   | 2832                               | 32.238                     |                        | 0.023   | 2790                               | 19.581                     |                        | 0.023 |
| $^{4}S_{3/2} \rightarrow ^{4}I_{15/2}$   | 18320                              | 389.280                    | 1.479                  | 0.576   | 18372                              | 258.421                    | 2.225                  | 0.575 |
| $\rightarrow$ <sup>4</sup> $I_{13/2}$  | 11775                              | 160.809                    |                        | 0.238   | 11820                              | 106.969                    |                        | 0.238 |
|  | 8089                               | 75.886                     |                        | 0.112   | 8147                               | 50.820                     |                        | 0.113 |
| $\rightarrow$ <sup>4</sup> $I_{9/2}$   | 5850                               | 39.686                     |                        | 0.059   | 5840                               | 26.108                     |                        | 0.058 |
| $\rightarrow$ $^4F_{9/2}$  | 3018                               | 10.563                     |                        | 0.016   | 3050                               | 7.121                      |                        | 0.016 |
| $^{2}\text{H}_{11/2} \rightarrow ^{4}\text{I}_{15/2}$  | 19195                              | 7293.147                   | 0.075                  | 0.550   | 19203                              | 4282.595                   | 0.129                  | 0.551 |
| $\rightarrow$ <sup>4</sup> $I_{13/2}$  | 12650                              | 3167.365                   |                        | 0.239   | 12651                              | 1858.777                   |                        | 0.239 |
| $\rightarrow$ <sup>4</sup> $I_{11/2}$  | 8964                               | 1590.403                   |                        | 0.120   | 8978                               | 936.158                    |                        | 0.120 |
| $\rightarrow$ <sup>4</sup> $I_{9/2}$   | 6725                               | 895.060                    |                        | 0.067   | 6671                               | 516.771                    |                        | 0.066 |
| $\rightarrow$ $^4F_{9/2}$  | 3893                               | 299.951                    |                        | 0.023   | 3881                               | 174.897                    |                        | 0.022 |
| $\rightarrow$ <sup>4</sup> S <sub>3/2</sub>  | 875                                | 15.155                     |                        | 0.001   | 831                                | 8.021                      |                        | 0.001 |
| <sup>4</sup> F <sub>2/2</sub> → <sup>4</sup> I <sub>15/2</sub>   | 20449                              | 1840.397                   | 0.280                  | 0.515   | 20501                              | 1200.092                   | 0.429                  | 0.514 |
| $\rightarrow$ <sup>4</sup> $I_{13/2}$  | 13904                              | 850.797                    |                        | 0.238   | 13950                              | 555.608                    |                        | 0.238 |
| $\rightarrow$ <sup>4</sup> $I_{11/2}$  | 10218                              | 459.479                    |                        | 0.129   | 10277                              | 301.545                    |                        | 0.129 |
| $ \begin{array}{c} 1//2 & I_{15/2} \\ \rightarrow^{4}I_{13/2} \\ \rightarrow^{4}I_{11/2} \\ \rightarrow^{4}I_{9/2} \\ \rightarrow^{4}F_{9/2} \end{array} $ | 7979                               | 280.157                    |                        | 0.078   | 7969                               | 181.327                    |                        | 0.078 |
| $\rightarrow$ $^4F_{9/2}$  | 5147                               | 116.580                    |                        | 0.033   | 5179                               | 76.589                     |                        | 0.033 |
| $\rightarrow$ $^4S_{3/2}$  | 2129                               | 19.948                     |                        | 0.006   | 2130                               | 12.948                     |                        | 0.033 |
| $\rightarrow$ <sup>2</sup> H <sub>11/2</sub>   | 1254                               | 6.920                      |                        | 0.002   | 1298                               | 4.814                      |                        | 0.002 |
| ${}^{4}F_{5/2} \rightarrow {}^{4}I_{15/2}$   | 22110                              | 690.752                    | 0.682                  | 0.471   | 22163                              | 458.027                    | 1.028                  | 0.471 |
| $\rightarrow$ <sup>4</sup> $I_{13/2}$  | 15564                              | 342.306                    |                        | 0.234   | 15612                              | 227.254                    |                        | 0.234 |
| $\rightarrow$ <sup>4</sup> $I_{11/2}$  | 11878                              | 199.369                    |                        | 0.136   | 11939                              | 132.902                    |                        | 0.137 |
|  | 9639                               | 131.286                    |                        | 0.090   | 9631                               | 86.491                     |                        | 0.089 |
| $\rightarrow$ <sup>4</sup> $F_{9/2}$   | 6807                               | 65.478                     |                        | 0.045   | 6841                               | 43.640                     |                        | 0.045 |
| $\rightarrow$ $^4S_{3/2}$  | 3789                               | 20.291                     |                        | 0.014   | 3792                               | 13.405                     |                        | 0.014 |
| $\rightarrow$ <sup>2</sup> H <sub>11/2</sub>   | 2914                               | 12.002                     |                        | 0.008   | 2961                               | 8.173                      |                        | 0.008 |
| $\rightarrow$ $^4F_{7/2}$  | 1660                               | 3.896                      |                        | 0.003   | 1662                               | 2.576                      |                        | 0.003 |

**Table 5** Value of  $\Omega_4/\Omega_6$  of different glass samples

| Table 5 value of 324/326 of different glass sa | ampies                |
|--|-----------------------|
| Glass sample                                   | $arOmega_4/arOmega_6$ |
| TZN (Present work)                             | 0.851                 |
| TZNBG 2 (Present work)                         | 0.783                 |
| TZNE 1 [6]                                     | 0.99                  |
| BT-70 [10]                                     | 2.09                  |
| BT-60 [10]                                     | 2.27                  |
| TW 1 [16]                                      | 2.03                  |
| TW 3 [16]                                      | 1.87                  |
| TCW 1 [16]                                     | 2.08                  |
| TCW 3 [16]                                     | 2.11                  |

$$\sigma_{\rm emis} = \frac{\lambda_{\rm p}^4}{8\pi c n^2 \Delta \lambda_{\rm eff}} A_{\rm ed}(J' \to J'')$$
 (5)

where  $\lambda_p$  is the peak fluorescence wavelength, and  $\Delta\lambda_{eff}$  is the effective line-width of emission band, which can be calculated using the following equation:

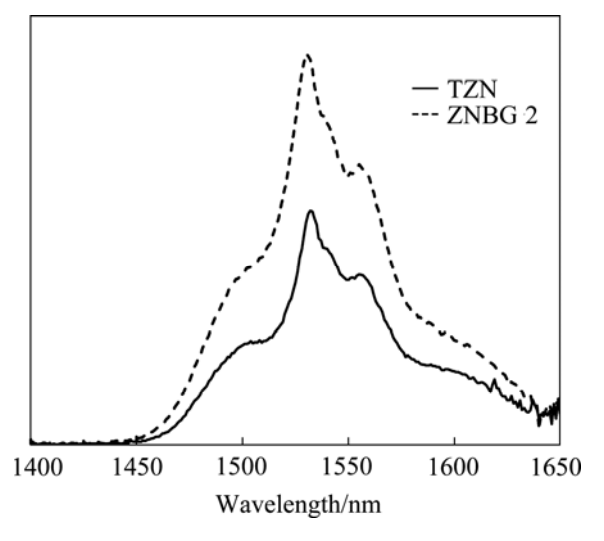


**Fig. 3** Emission spectra of  ${}^4I_{13/2}{\to}{}^4I_{15/2}$  transition of  $Er^{3+}$  in all glasses under 976 nm excitation

$$\Delta \lambda_{\text{eff}} = \frac{\int I(\lambda) d\lambda}{I_{\text{max}}} \tag{6}$$

where  $I_{\text{max}}$  is the maximum intensity at the fluorescence emission peak.

Table 6 gives the emission cross-section  $\sigma_{\rm emis}$ , and the full width at half maxima (FWHM) of the emission peak of  ${}^{4}I_{13/2} \rightarrow {}^{4}I_{15/2}$  transition of Er<sup>3+</sup> in different glass matrices. Bandwidth properties of the optical amplifier can be evaluated from the product of  $\sigma_{emis}$  and FWHM, and the larger the better. The value of  $\sigma_{\rm emis}\tau_{\rm i}$  can be applied to evaluating the gain of bandwidth [16]. As the results present in Table 6, these parameters of TZNBG 2 glass sample are more excellent than those of other glass sample. Further more, the value of  $\sigma_{\text{emis}} \times \text{FWHM}$  of tellurite glass samples that introduced B<sub>2</sub>O<sub>3</sub> and GeO<sub>2</sub> is larger than TZN glass samples too [7,17]. On the other hand, the product of  $\sigma_{\rm emis}$  and  $\tau_{\rm i}$  is the largest among these glass samples. So, the tellurite glass samples contain B<sub>2</sub>O<sub>3</sub> and GeO<sub>2</sub> are more suitable to be used as candidate for broad band optical amplifiers.

**Table 6** Emission cross-section  $\sigma_{emis}$ , FWHM and radiative lifetime  $\tau_i$  of  ${}^4I_{13/2} {\longrightarrow} {}^4I_{15/2}$  transition of  $Er^{3+}$  in different glass samples

| samples  |             |         |   |  |
|--|-------------|---------|---|--|
| Glass sample   | FWHM/<br>nm | ~ CHIIS | $\sigma_{\text{emis}} \times \text{FWHM}/$ $(10^{-21} \text{cm}^2 \cdot \text{nm})$ | $\frac{\sigma_{\rm emis}\tau_{\rm i}}{(10^{-21}{\rm cm}^2{\rm \cdot ms})}$ |
| TZN<br>(Present<br>work)   | 52          | 3.984   | 207.168   | 30.669   |
| TZNBG 2<br>(Present<br>work)   | 58          | 8.151   | 472.758   | 108.474  |
| TZNE 1[6]  | 58          | 2.404   | 139.43  | 9.469  |
| 70TeO <sub>2</sub> -<br>15ZnO-<br>15Na <sub>2</sub> O-<br>0.1Er <sub>2</sub> O <sub>3</sub><br>[15]  |             |         | 332.7   | 0.0037   |
| 5Na <sub>2</sub> O-<br>20Sb <sub>2</sub> O <sub>3</sub> -<br>35B <sub>2</sub> O <sub>3</sub> -<br>39SiO <sub>2</sub> -<br>1Er <sub>2</sub> O <sub>3</sub> [18] | 88          | 6.8     | 598.4   | 25.976   |

### **4 Conclusions**

- 1) The results of DSC and thermal mechanical analysis reveal that  $Er^{3+}$ -doped TZNBG glasses possess high thermal stability, the  $\Delta T$  is higher than 134 °C and the  $\alpha$  is in the range of  $(10.938-12.279)\times10^{-6}$ °C.
- 2) The value of  $\Omega_4/\Omega_6$  is estimated to be 0.783 for  $\mathrm{Er}^{3+}$  in TZNBG glass sample, which indicates that the

transition  ${}^4I_{13/2} \rightarrow {}^4I_{15/2}$  is more efficient than that in other glass samples. The emission cross-section  $\sigma_{emis}$ , and FWHM of 1530 nm emission peak of  ${}^4I_{13/2} \rightarrow {}^4I_{15/2}$  transition of the Er<sup>3+</sup> suggest that the TZNBG glass samples have good bandwidth properties and high gain of bandwidth.

3) On the basis of all the data obtained, the thermal stability and optical properties of Er<sup>3+</sup>-doped TZNBG glasses are improved.

#### References

- WANG J S, VOGEL E M, SNITZER E. Tellurite glass: A new candidate for fiber devices [J]. Optical Materials, 1994, 3: 187–203.
- [2] WEBER M J, MYERS J D, BLACKBURN D H. Optical properties of Nd<sup>3 +</sup> in tellurite and phosphotellurite glasses [J]. Journal of Applied Physics, 1981, 52: 2944–2949.
- [3] BERNESCHI S, NUNZI CONTI G, BÁNYÁSZ I, KHANH N Q, FRIED M, PÁSZTI F, BRENCI M, PELLI S, RIGHINI G C. Ion beam irradiated channel waveguides in Er<sup>3+</sup>-doped tellurite glass [J]. Applied Physics Letters, 2007, 90: 121136.
- [4] XIANG Shen, NIE Qiu-hua, XU Tie-feng, DAI Shi-xun, WANG Xun-si. Effect of B<sub>2</sub>O<sub>3</sub> on luminescence of erbium doped tellurite glasses [J]. Spectrochimica Acta Part A, 2007, 66: 389–393.
- [5] RIVERA V A G, RODRIGUEZ E, CHILLCCE E F, CESAR C L, BARBOSA L C. Waveguide produced by fiber on glass method using Er<sup>3+</sup>-doped tellurite glass [J]. Journal of Non-Crystalline Solids, 2007, 353: 339–343.
- [6] JLASSI I, ELHOUICHET H, FARTHOU M. Judd-Ofelt analysis and improvement of thermal and optical properties tellurite glasses by adding P<sub>2</sub>O<sub>5</sub> [J]. Journal of Luminescence, 2010, 130: 2394–2401.
- [7] EL-MALLAWANY R, ABBAS AHMED I. Thermal properties of multicomponent tellurite glass [J]. Journal of Materials Science, 2008, 43: 5131-5138.
- [8] HRUBY A. Evaluation of glass-forming tendency by means of DTA[J]. Czech Journal of Physics B, 1972, 22: 1187–1193.
- [9] DREXHAGE M G, EI BAYOUMI O H, MOYNIYAN C T. Preparation and properties of heavy-metal fluoride glasses containing ytterbium or lutetium [J]. Journal of the American Ceramic Society C, 1982, 65: 168–171.
- [10] JOSHI P, SHEN Shao-xiong, JHA A. Er<sup>3+</sup>-doped boro-tellurite glass for optical amplification in the 1530–1580 nm [J]. Journal of Applied Physics, 2008, 103: 083543.
- [11] JUDD B R. Optical absorption intensities of rare-earth ions [J]. Physical Review, 1962, 127: 750-761.
- [12] OFELT G S. Intensities of crystal spectra of rare-earth ions [J]. Journal of Chemical Physics, 1962, 37: 511–520.
- [13] CARNALL W T, P R F, RAJNAK K. Electronic energy levels in the trivalent lanthanide aquo ions: I. Pr<sup>3+</sup>, Nd<sup>3+</sup>, Pm<sup>3+</sup>, Sm<sup>3+</sup>, Dy<sup>3+</sup>, HO<sup>3+</sup>, Er<sup>3+</sup>and Tm<sup>3+</sup> [J]. Journal of Chemical Physics, 1968. 49(10): 4424–4442.
- [14] JACOBS R R, WEBER M J. Dependence of the  ${}^4F_{3/2} \rightarrow {}^4I_{11/2}$  induced-emission cross section for Nd<sup>3+</sup> on glass composition [J]. IEEE Journal of Quantum Electron, 1976, 12: 102–111.
- [15] YU Chun-lei, HE Dong-bing, WANG Guo-nian, ZHANG Jun-jie,
   HU Li-li. Influence of cationic field strength of modifiers on the 1.53
   μm spectroscopic properties of Er<sup>3+</sup>-doped tellurite glasses [J].

 $\label{pour normal of Non-Crystalline Solids, 2009, 355: 2250-2253.}$ 

- [16] BILIR G, OZEN G, TATAR D, ÖVEÇOğLU M L. Judd-Ofelt analysis and near infrared emission properties of the  $Er^{3+}$  ions in tellurite glasses containing WO<sub>3</sub> and CdO [J]. Optics Communications, 2011, 284: 863–868.
- [17] McCUMBER D E. Theory of phonon-terminated optical masers [J].

Physical Review A, 1964, 134: 299-306.

[18] QIAN Q, WANG Y, ZHANG Q Y, YANG G F, YANG Z M, JIANG Z H. Spectroscopic properties of Er<sup>3+</sup>-doped Na<sub>2</sub>O-Sb<sub>2</sub>O<sub>3</sub>-B<sub>2</sub>O<sub>3</sub>-SiO<sub>2</sub> glasses [J]. Journal of Non-Crystalline Solids, 2008, 354: 1981–1985.

## 掺铒碲酸盐的热稳定性和 Judd-Ofelt 理论分析

任 芳,梅宇钊,高 超,朱立刚,卢安贤

中南大学 材料科学与工程学院,长沙 410083

摘 要:利用熔融法制备掺铒  $TeO_2$ –ZnO– $Na_2O$ – $B_2O_3$ – $GeO_2$  碲酸盐玻璃。采用差热扫描分析法(DSC)和热分析 (TMA)得到玻璃的玻璃转化温度( $T_g$ )、玻璃析晶温度( $T_x$ )、玻璃软化温度( $T_f$ )和热膨胀系数( $\alpha$ ),应用 Judd-Ofelt 理论计算玻璃中  $Er^{3+}$ 的振子强度 $\Omega_{\lambda}$  ( $\lambda$ =2, 4, 6),跃迁几率  $A_{ed}$ ,荧光分支比  $\beta$ ,辐射寿命  $\tau_i$ 。根据 McCumber 理论计算  $Er^{3+}$ 离子  $^4I_{13/2}$  $\rightarrow ^4I_{15/2}$ 的受激发射截面  $\sigma_{emis}$ 和荧光半高宽 FWHM。得出此体系的玻璃具有高热稳定性和低热膨胀性,具有较高的  $Er^{3+}$ 离子  $^4I_{13/2}$  $\rightarrow ^4I_{15/2}$  能级跃迁效率和较好的增益带宽性能。

关键词: 碲酸盐玻璃; 热稳定性; Judd-Ofelt 理论; 光谱性能

(Edited by LI Xiang-qun)